Observation of phononic helical edge states in a mechanical topological insulator

R. Süsstrunk and, S. Huber, Science **349**, 6243 (2015)
[DOI:10.1126/science.aab0239]

A topological insulator, as originally proposed for electrons governed by quantum mechanics, is characterized by a dichotomy between the interior and the edge of a finite system: The bulk has an energy gap, and the edges sustain excitations traversing this gap. However, it has remained an open question whether the same physics can be observed for systems obeying Newtons equations of motion. We conducted experiments to characterize the collective behavior of mechanical oscillators exhibiting the phenomenology of the quantum spin Hall effect. The phononic edge modes are shown to be helical, and we demonstrate their topological protection via the stability of the edge states against imperfections. Our results may enable the design of topological acoustic metamaterials that can capitalize on the stability of the surface phonons as reliable wave guides.

The main idea

- A QM lattice problem

$$i\hbar\dot{\psi}_i^\alpha = \mathcal{H}_{ij}^{\alpha\beta}\psi_j^\beta$$

α-spin, i-lattice site, $\mathcal{H}_{ij}^{\alpha\beta}$ QSHE Hamiltonian

The main idea

- A QM lattice problem

$$i\hbar\dot{\psi}_i^\alpha = \mathcal{H}_{ij}^{\alpha\beta}\psi_j^\beta$$

α-spin, i-lattice site, $\mathcal{H}_{ij}^{\alpha\beta}$ QSHE Hamiltonian

- Classical harmonic oscillators

$$\ddot{x}_i = -\mathcal{D}_{ij}x_j$$

x_i coordinates of N pendulums, $\mathcal{D}_{ij}$ is the real, symmetric, positive definite matrix.

The main idea

- A QM lattice problem

$$i\hbar\dot{\psi}_i^{\alpha} = \mathcal{H}_{ij}^{\alpha\beta}\psi_j^{\beta}$$

  α-spin, i-lattice site, $\mathcal{H}_{ij}^{\alpha\beta}$ QSHE Hamiltonian

- Classical harmonic oscillators

$$\ddot{x}_i = -\mathcal{D}_{ij}x_j$$

  x_i coordinates of N pendulums, $\mathcal{D}_{ij}$ is the real, symmetric, positive definite matrix.

- Existence and properties of edge modes are features of $\mathcal{H}$ or $\mathcal{D} \rightarrow$ independent of the interpretation of ψ_i^{α} versus x_i or the nature of the dynamics ($i\partial t$ vs. $\partial^2 t$)

The main idea

- A QM lattice problem
$$i\hbar\dot{\psi}_i^\alpha = \mathcal{H}_{ij}^{\alpha\beta}\psi_j^\beta$$
α-spin, i-lattice site, $\mathcal{H}_{ij}^{\alpha\beta}$ QSHE Hamiltonian
- Classical harmonic oscillators
$$\ddot{x}_i = -\mathcal{D}_{ij}x_j$$
x_i coordinates of N pendulums, $\mathcal{D}_{ij}$ is the real, symmetric, positive definite matrix.
- Existence and properties of edge modes are features of $\mathcal{H}$ or $\mathcal{D}$ $\rightarrow$ independent of the interpretation of ψ_i^α versus x_i or the nature of the dynamics ($i\partial t$ vs. $\partial^2 t$)
- Authors map a QM QSHE system to a mechanical system of oscillators and show experimentally the existence of edge modes and their topological properties.

QM model

- Starting with two independent copies of Hofstadter model (fermions hopping on a 2D square lattice in a B-field with $\Phi = \Phi_S/S = 2\pi/3$ flux per plaquette)

$$\mathcal{H} = \sum_{\alpha=\pm} \mathcal{H}_{\alpha,\Phi} = \begin{pmatrix} \mathcal{H}_\Phi & 0 \\ 0 & \mathcal{H}_\Phi^* \end{pmatrix} .$$

- where

$$\mathcal{H}_{\alpha,\Phi} = f_0 \sum_{r,s} |r,s,\alpha\rangle\langle r,s\pm 1,\alpha| + |r,s,\alpha\rangle\langle r\pm 1,s,\alpha| e^{\pm i\alpha\Phi_S}$$

QM model

$$\mathcal{H}_{\alpha,\Phi} = f_0 \sum_{r,s} |r,s,\alpha\rangle\langle r,s\pm 1,\alpha| + |r,s,\alpha\rangle\langle r\pm 1,s,\alpha| e^{\pm i\alpha\Phi_S}$$

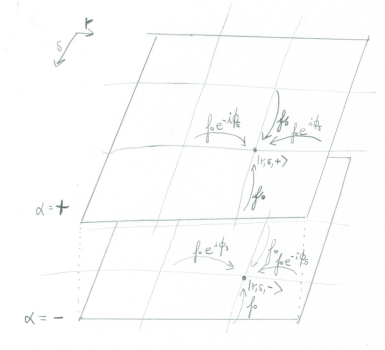

- The model yields three doubly degenerate bands separated by non-zero gaps with one helical edge state per pseudo-spin.

Identification with a classical system

- $\mathcal{H}$ is complex $\to$ change of basis (combining local Kramer's pairs):

$$\left(\begin{array}{c} x_{r,s} \\ y_{r,s} \end{array} \right) = \underbrace{\sqrt{2} \left(\begin{array}{cc} 1 & -i \\ 1 & i \end{array} \right)^{-1}}_{u^{-1} \to U = u \otimes 1_{textlattice}} \left(\begin{array}{c} \psi^{+}_{r,s} \\ \psi^{-}_{r,s} \end{array} \right) .$$

- Hence

$$U^{\dagger} \mathcal{H} U = \left(\begin{array}{cc} Re\mathcal{H}_{\Phi} & Im\mathcal{H}_{\Phi} \\ Im\mathcal{H}_{\Phi} & Re\mathcal{H}_{\Phi} \end{array} \right) \equiv \mathcal{D}$$

- Correspondence: QM pseudospin $\alpha \leftrightarrow$ circular polarization of the pendulum

Experimental realization

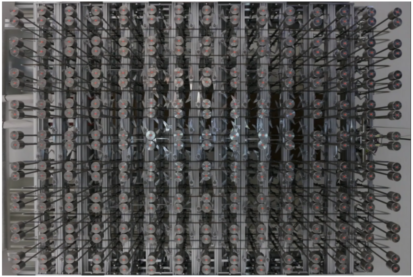

View from the bottom

- sites: $L_r \times L_s = 9 \times 15$, 2 pendulums per site (x and y mode)

Experimental realization

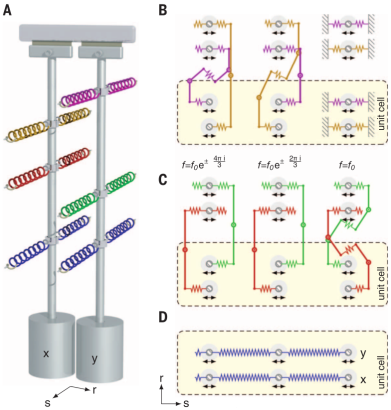

- x-x, y-y, x-y coupling is implemented according to $\mathcal{D}$ matrix.

Experimental realization

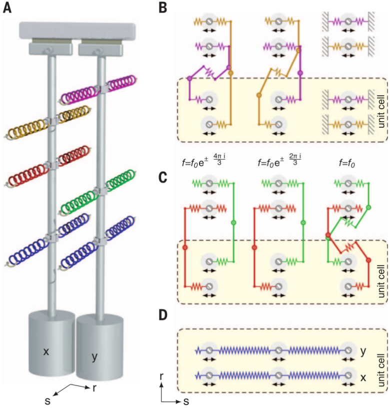

- x-x, y-y, x-y coupling is implemented according to $\mathcal{D}$ matrix.
- 3.mov

Analyzing the system

- Harmonically excite one site with a well-defined polarization.

Analyzing the system

- Harmonically excite one site with a well-defined polarization.
- 1.mov

Analyzing the system

- Harmonically excite one site with a well-defined polarization.
- 1.mov
- Tracking the positions of all pendulums they obtain $[x_{r,s}(t), y_{r,s}(t)] \rightarrow$ amplitude $A_{r,s}$ and the polarization (the lag between x and y pendulums).

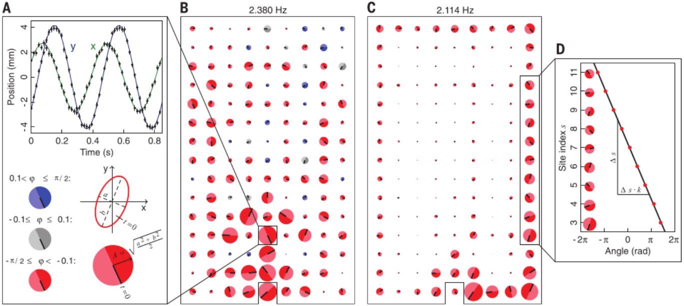

Edge states

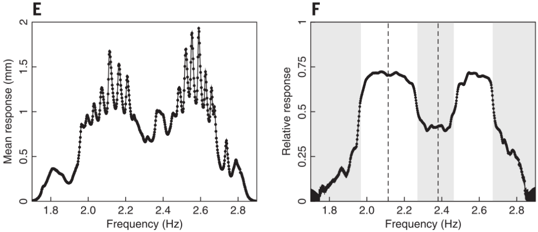

- Total response $\chi = \sum_{r,s} A_{r,s}/N$ (overall band width 1.7 Hz - 2.9 Hz)

Edge states

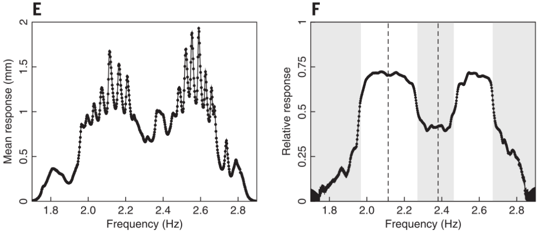

- Total response $\chi = \sum_{r,s} A_{r,s}/N$ (overall band width 1.7 Hz - 2.9 Hz)
- Relative response $\chi_e/(\chi_b + \chi_e)$ where $\chi_e = \sum_{\text{edge}} A_{r,s}/N_{\text{edge}}$ and $\chi_b = \sum_{\text{bulk}} A_{r,s}/N_{\text{bulk}}$
- In the two frequency regions (white) the response is dominated by edge modes.

Edge states

- Structure of the 2 highlighted modes from Fig.F

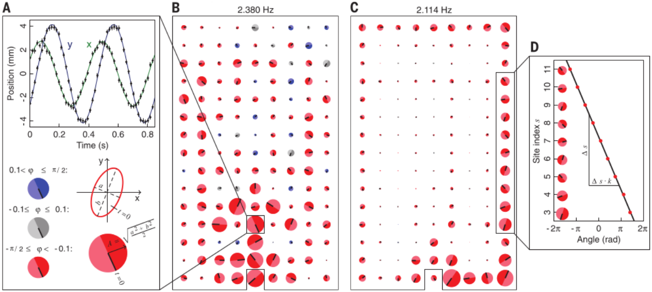

Are the edge states helical?

- In analogy to the QSHE the edge states are expected to be helical.

Are the edge states helical?

- In analogy to the QSHE the edge states are expected to be helical.
- The wave vector along the edge is extracted from the steady state

$$k = \phi_{r,s+1} - \phi_{r,s}$$

where $\phi_{r,s}$ is the angle of the vector $[x_{r,s}(t_0), y_{r,s}(t_0)]$ w.r.t. the positive x-direction.

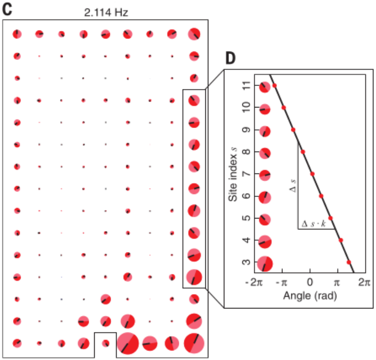

Are the edge states helical?

- Scanning the edge state frequencies and extracting the wave vectors and polarization → dispersion $\omega(k)$

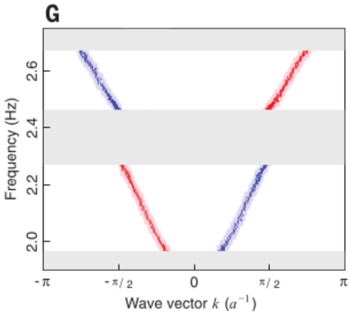

- For each polarization there is an unidirectional mode per gap as expected.

Symmetry protected edge states, polarizing beam splitter

- Helicity of the edge dispersion ⇒ the edge states act as a polarizing beam splitter.

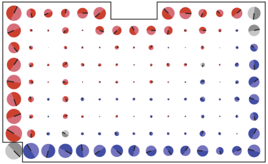

Symmetry protected edge states, polarizing beam splitter

- Helicity of the edge dispersion $\Rightarrow$ the edge states act as a polarizing beam splitter.

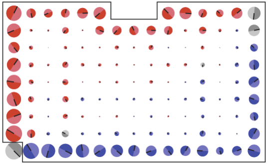

- The QSHE is protected by the QM time-reversal (TR) symmetry.

Symmetry protected edge states, polarizing beam splitter

- Helicity of the edge dispersion $\Rightarrow$ the edge states act as a polarizing beam splitter.

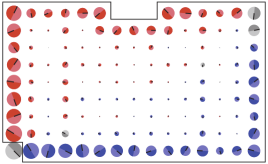

- The QSHE is protected by the QM time-reversal (TR) symmetry.
- Corresponding symmetry in this classical system is

$$\{t \to -t\} \circ \{(x_{r,s}, y_{r,s}) \to (y_{r,s}, -x_{r,s})\}$$

and can be broken by disorder on the local couplings.

Symmetry protected edge states, polarizing beam splitter

- Helicity of the edge dispersion ⇒ the edge states act as a polarizing beam splitter.

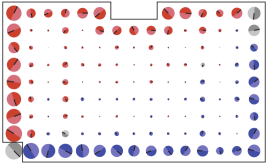

- The QSHE is protected by the QM time-reversal (TR) symmetry.
- Corresponding symmetry in this classical system is

$$\{t \to -t\} \circ \{(x_{r,s}, y_{r,s}) \to (y_{r,s}, -x_{r,s})\}$$

  and can be broken by disorder on the local couplings.
- Analyzing the efficiency of the system as a beam splitter ⇒ on the length scale of the system the symmetry breaking disorder is irrelevant. (i.e. the symmetry is preserved)

Are the edge states robust?

- Exact shape of the boundary has no influence on the stability of the edge states:

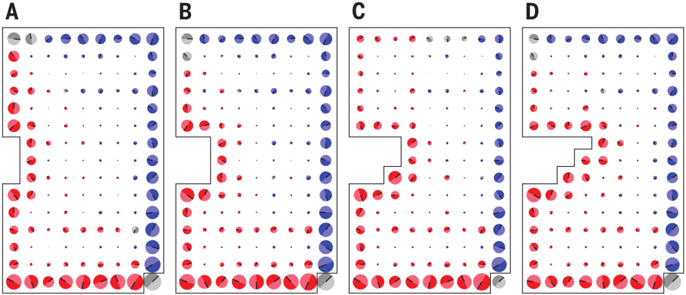

Are the edge states robust? Domain wall

- The edge states are not just a result of the finite-size geometry.

Are the edge states robust? Domain wall

- The edge states are not just a result of the finite-size geometry.
- A domain wall is created inverting the effective flux on six rows of the system:

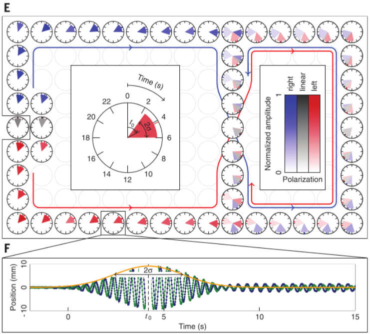

Conclusions

- Measured edge spectrum, the efficiency of the edge states as a beam splitter and their immunity to surface roughness ⇒ QSHE phenomenology can be implemented in an imperfect mechanical system.

Conclusions

- Measured edge spectrum, the efficiency of the edge states as a beam splitter and their immunity to surface roughness $\Rightarrow$ QSHE phenomenology can be implemented in an imperfect mechanical system.
- Dissipation of the mechanical energy $\rightarrow$ quality factor Q. The chirality of edge states leads to a decay length $\xi \sim Q$ (bidirectional wave guide $\xi \sim \sqrt{Q}$ (random walk)).

Conclusions

- Measured edge spectrum, the efficiency of the edge states as a beam splitter and their immunity to surface roughness $\Rightarrow$ QSHE phenomenology can be implemented in an imperfect mechanical system.
- Dissipation of the mechanical energy $\rightarrow$ quality factor Q. The chirality of edge states leads to a decay length $\xi \sim Q$ (bidirectional wave guide $\xi \sim \sqrt{Q}$ (random walk)).
- Although the experiment was performed with coupled pendulums, the mapping $\mathcal{H} \rightarrow \mathcal{D}$ is more general and can be used to design acoustic metamaterials.

Efficiency of the beam splitter

- Analyzing the efficiency of the system as a beam splitter they conclude that on the length scale of the system the symmetry breaking disorder is irrelevant. (i.e. the symmetry is preserved)

Fig. 3. Beam splitter. (**A**) Geometry of the beam splitter. An arbitrary polarization is injected at the excluded edge site at 2.123 Hz. The relative weights *A* on the two shaded boxes L and R define a splitting ratio. (**B**) Splitting ratio on the Poincaré sphere. The north and south poles of the sphere respectively correspond to right and left circular polarizations of the drive. The color map is an interpolation based on 7000 data points. The maximal splitting is not reached at the poles, indicating the presence of disorder. The dots mark measurements along a great circle through the points of maximal splitting. (**C**) Splitting ratio along the great circle shown in (B). The black line marks a cosine expected for an optimal beam splitter. The maximally reached splitting is 99.80 ± 0.04%.